

## Estimation of the air/sea exchange of ammonia for the North Atlantic Basin

P.K. QUINN<sup>1</sup>, K.J. BARRETT<sup>2</sup>, F.J. DENTENER<sup>3</sup>, F. LIPSCHULTZ<sup>4</sup> & K.D. SIX<sup>5</sup>

<sup>1</sup>NOAA Pacific Marine Environmental Laboratory, Seattle, WA, USA; <sup>2</sup>Norwegian Meteorological Institute, Oslo, Norway; <sup>3</sup>Wageningen Agricultural University, Wageningen, Netherlands; <sup>4</sup>Bermuda Biological Station for Research, Bermuda; <sup>5</sup>Max-Planck-Institute for Meteorology, Hamburg, Germany

Received 19 December 1994; accepted 6 March 1996

**Abstract.** As gas phase atmospheric ammonia reacts with acidic aerosol particles it affects the chemical, physical, and optical properties of the particles. A knowledge of the source strengths of  $\text{NH}_3$  is useful in determining the effect of  $\text{NH}_3$  on aerosol properties on a regional basis. Here, an attempt is made to determine the direction and magnitude of the air/sea flux of ammonia for the North Atlantic Basin from both measured and modeled seawater and atmospheric ammonia concentrations. Previously reported measured seawater concentrations range from less than 30 to 4600 nM with the highest concentrations reported for the Caribbean Sea, the North Sea, and the Belgium coast. Measured atmospheric ammonia concentrations range from 2 to 500 nmol m<sup>-3</sup> with the largest values occurring over the Sargasso Sea, the Caribbean Sea, and the North Sea. For comparison to the measurements, seawater ammonia concentrations were calculated by the Hamburg Model of the Ocean Carbon Cycle (HAMOCC3). HAMOCC3 open ocean values agree well with the limited number of reported measured concentrations. Calculated coastal values are lower than those measured, however, due to the coarse resolution of the model. Atmospheric ammonia concentrations were calculated by the Acid Deposition Model of the Meteorological Synthesizing Center (MSC-W) and by the global 3-dimensional model Moguntia. The two models predict similar annually averaged values but are about an order of magnitude lower than the measured concentrations. Over the North Sea and the NE Atlantic, the direction and magnitude of the air/sea ammonia flux calculated from MSC-W and Moguntia agree within the uncertainty of the calculations. Flux estimates derived from measured data are larger in both the positive and negative direction than the model derived values. The discrepancies between the measured and modeled concentrations and fluxes may be a result of sampling artifacts, inadequate chemistry and transport schemes in the models, or the difficulty in comparing point measurements to time-averaged model values. Sensitivity tests were performed which indicate that, over the range of values expected for the North Atlantic, the accuracy of the calculated flux depends strongly on seawater and atmospheric ammonia concentrations. Clearly, simultaneous and accurate measurements of seawater and atmospheric ammonia concentrations are needed to reduce the uncertainty of the flux calculations, validate the model results, and characterize the role of oceanic ammonia emissions in aerosol processing and nitrogen cycling for the North Atlantic.

### 1. Introduction

In the marine atmosphere, gas phase acidic species that can act as aerosol particle precursors include  $\text{H}_2\text{SO}_4$ ,  $\text{HNO}_3$  and organic acids. Because gas

phase ammonia,  $\text{NH}_3$  (g), is the dominant basic species available to interact with these acidic compounds, it has a unique role in determining the chemical, physical, and optical properties of both marine and continental aerosol. It can have a significant impact on the formation of new particles by lowering the vapor concentration of other gases required for the initiation of nucleation. It also can result in particle growth by reacting with acidic particles and lowering the surface acid vapor pressure thereby enhancing the condensation of gas phase acidic species. In addition, the degree of neutralization of non-seasalt sulfate aerosol by  $\text{NH}_3$  (g) will influence the aerosol hygroscopicity and, hence, the growth response of particles to changes in atmospheric relative humidity. As light scattering by aerosol particles is determined, in part, by the size dependent aerosol mass concentration,  $\text{NH}_3$  (g) will influence the scattering efficiency of the aerosol by adding particulate mass and by changing its hygroscopic properties.

A knowledge of the sources of  $\text{NH}_3$  (g) as well as their magnitude is needed to determine the spatial and temporal variability of the effect of  $\text{NH}_3$  (g) on aerosol chemical, physical, and optical properties. Much work has been reported on quantifying the sources of  $\text{NH}_3$  (g) in continental regions (e.g., Buijsman et al. 1987; Asman et al. 1988). Comparatively little research has been done, however, in characterizing the direction and magnitude of the ammonia flux in oceanic regions. Hence, the importance of the oceanic source of  $\text{NH}_3$  on global and regional scales is unknown as is the impact of continental sources on oceanic regions. The goal of the present work is to determine the direction and magnitude of the air/sea ammonia flux for different regions of the North Atlantic and for continental regions bordering the Atlantic. The deposition of ammonium to the sea surface and its importance in ocean processes is described in a separate article (Prospero et al., this issue).

$\text{NH}_3$  (g) reacts primarily with submicron non-seasalt sulfate aerosol, nss  $\text{SO}_4^{2-}$  (p), to form ammoniated sulfate salts ranging in composition from  $\text{NH}_4\text{HSO}_4$  to  $(\text{NH}_4)_2\text{SO}_4$  (Quinn et al. 1987). In remote ocean regions, the major source of atmospheric  $\text{NH}_3$  will be the ocean itself (Quinn et al. 1988, 1990). In coastal regions,  $\text{NH}_3$  (g) also may be derived from continental sources such as biomass burning, animal wastes, emissions from soil and vegetation, and fertilizer losses (Dentener & Crutzen 1994; Warneck 1988). Both the ocean- and the continentally-derived  $\text{NH}_3$  (g) will react with unneutralized sulfate aerosol. The resulting particulate phase ammonium,  $\text{NH}_4^+$  (p), may be transported long distances (100's to 1000's of miles depending on prevailing wind speeds and precipitation frequency) before it is removed from the atmosphere through wet and dry deposition.

Ammonia exists in seawater as both ionized ammonium,  $\text{NH}_4^+$  (s), and dissolved ammonia,  $\text{NH}_3$  (s).  $\text{NH}_3$  (s) contributes about 10% to the total

seawater ammonium concentration,  $\text{NH}_x(\text{s})$ , at a pH of 8.2 and temperature of 25 °C.  $\text{NH}_x(\text{s})$  is produced in the upper ocean from the degradation of organic nitrogen containing compounds and excretion from zooplankton. It also is released from bottom sediments to overlying waters. Loss processes for  $\text{NH}_x(\text{s})$  include bacterial nitrification, uptake by phytoplankton and bacteria, and emission across the air/sea interface. It is the unionized dissolved form,  $\text{NH}_3(\text{s})$ , that is exchanged across the ocean surface and serves as a source of atmospheric ammonia. At steady state, an equilibrium is reached between air and seawater concentrations of ammonia so that both  $\text{NH}_3(\text{s})$  and  $\text{NH}_3(\text{g})$  determine the direction and magnitude of the air/sea flux.

Attempts to estimate the air/sea flux of ammonia for the North Atlantic Basin are hindered by a lack of simultaneous measurements of oceanic and atmospheric concentrations. This lack of measurements can be attributed to the difficulty in determining very low concentrations of  $\text{NH}_3(\text{g})$  using currently available techniques and in avoiding sample contamination (Williams et al. 1992). Similarly,  $\text{NH}_x(\text{s})$  concentrations frequently are below the detection limits (50 to 100 nM) of conventional techniques (D'Elia 1983). The result is that little is known about the magnitude and direction of the air/sea ammonia flux. Only one study from the North Atlantic Basin which took place in the North Sea reports results of simultaneously determined  $\text{NH}_3(\text{g})$  and  $\text{NH}_x(\text{s})$  concentrations (Asman et al. 1994). From these measurements, it was determined that there is a variable net flux of ammonia ranging from  $-75$  to  $43 \mu\text{mol m}^{-2} \text{d}^{-1}$  where negative values indicate a flux from the atmosphere to the ocean. The direction of the flux appears to depend on the highly variable atmospheric  $\text{NH}_3(\text{g})$  concentrations. This variability is, in turn, a result of the proximity of the measurements to continental source regions.

Simultaneous measurements of  $\text{NH}_3(\text{g})$  and  $\text{NH}_3(\text{s})$  from the central and NE Pacific Ocean indicate that there is a net flux of ammonia from the ocean to the atmosphere ranging between  $1.8$  and  $16 \mu\text{mol m}^{-2} \text{d}^{-1}$  (Quinn et al. 1988, 1990). Based on observations of an increasing  $\text{NH}_4^+(\text{p})$  to  $\text{nss SO}_4^{2-}(\text{p})$  molar ratio, Clarke & Porter (1993) have inferred a similar efflux of ammonia from the ocean to the atmosphere of about  $10 \mu\text{mol m}^{-2} \text{d}^{-1}$  over the equatorial Pacific. These few measurements from the North Sea and the Pacific Ocean indicate that the ocean may serve as a local source of  $\text{NH}_3$  in remote regions but that there will be a net deposition to the surface in regions impacted by continental sources.

In this paper, we estimate regional air/sea fluxes of ammonia from reported measurements of  $\text{NH}_3(\text{g})$  and  $\text{NH}_x(\text{s})$ . We then compare these measurement-derived fluxes with those estimated from two sets of model calculations. The two models used are the Acid Deposition Model of the Meteorological

Table 1. Notation used for ammonia species in the marine environment.

Species	Notation	Concentration notation
Atmospheric gas phase $\text{NH}_3$	$\text{NH}_3$ (g)	$(\text{NH}_3)_g, \text{nmol m}^{-3}$
Atmospheric particulate phase $\text{NH}_4^+$	$\text{NH}_4^+$ (p)	$(\text{NH}_4^+)_p, \text{nmol m}^{-3}$
Seawater total $\text{NH}_3$ and $\text{NH}_4^+$	$\text{NH}_x$ (s)	$[\text{NH}_x]_s, \text{nM}$
Seawater dissolved, unionized $\text{NH}_3$	$\text{NH}_3$ (s)	$[\text{NH}_3]_s, \text{nM}$
$\text{NH}_3$ in equilibrium with dissolved $\text{NH}_3$ in the sea surface	$\text{NH}_3$ (s,eq)	$(\text{NH}_3)_{s,\text{eq}}, \text{nmol m}^{-3}$

Synthesizing Center-West of EMEP (MSC-W) (Tuovinen et al. 1994) and the global atmospheric transport/chemistry model Moguntia (Dentener & Crutzen 1994; and references therein) together with the Hamburg Model of the Ocean Carbon Cycle (HAMOCC3) (Kurz 1993). The sensitivity of the flux calculation to changes in surface seawater temperature, pH, salinity, and  $\text{NH}_x$  (s) and  $\text{NH}_3$  (g) concentrations also is determined.

## 2. Model descriptions

### 2a. *Moguntia* and *HAMOCC3* models

Moguntia, a global transport model of the troposphere, has a horizontal resolution of 10 by 10 degrees and 10 vertical layers which are spaced every 100 hPa. It uses monthly averaged winds and an eddy-diffusion parameterization based on the standard deviations of the winds together with a parameterization for deep cumulus convection. A complete description of the use of Moguntia to simulate the global atmospheric  $\text{NH}_3$  cycle is given by Dentener & Crutzen (1994).

In the model,  $\text{NH}_3$  (g) is removed from the atmosphere through wet and dry deposition and reaction with acidic sulfate aerosols and cloud droplets. Moguntia-calculated values of ammonium deposition in the North Atlantic basin are presented by Prospero et al. (this issue).  $\text{NH}_3$  (g) is allowed to react with sulfuric acid aerosol until an  $\text{NH}_4^+$  (p) to non-seasalt  $\text{SO}_4^{2-}$  (p) molar ratio of 1.5 is reached. This neutralization limit is motivated by the possibility that the equilibrium vapor pressure over nearly-neutralized sulfate aerosols may be substantial. The formation of particulate phase  $\text{NH}_4\text{NO}_3$  occurs primarily in continental regions where there are high concentrations of  $\text{HNO}_3$  (g) and  $\text{NH}_3$  (g). Due to the large spatial scales of Moguntia, the formation of  $\text{NH}_4\text{NO}_3$  is not included in this work. Omission of  $\text{NH}_4\text{NO}_3$  may add uncertainty to the calculated flux of  $\text{NH}_3$  to the ocean surface. This uncertainty is assumed to be negligible, however, as calculations with the

more detailed MSC-W of EMEP model (see Section 2b) indicate that only a small fraction of the aerosol exists as  $\text{NH}_4\text{NO}_3$ . The air/sea flux of  $\text{NH}_3$  is calculated using  $\text{NH}_x$  (s) concentrations estimated by HAMOCC3 and the method described in Section 5a. In the previous work of Dentener & Crutzen (1994),  $\text{NH}_3$  fluxes were scaled to those of DMS. In this work, however, calculated oceanic  $\text{NH}_3$  concentrations and piston velocities are used.

The global ocean circulation model HAMOCC3 has a horizontal resolution of 3.5 by 3.5 degrees and 15 vertical layers with a finer resolution in the upper 350 m (Maier-Reimer et al. 1993). The model operates on a monthly time step. It originally was designed to simulate the global marine carbon cycle and has been modified to include a simplified plankton model (Kurz 1993). Processes taken into account include the uptake of  $\text{NH}_x$  (s) by phytoplankton, regeneration of  $\text{NH}_x$  (s) by grazers, and bacterial utilization of  $\text{NH}_x$  (s). Monthly averaged exchange velocities are calculated from 6 hour ECMWF windfields following the method of Duce et al. (1991). A complete description of the use of HAMOCC3 to model the air/sea exchange of  $\text{NH}_3$  is given by Kurz & Dentener (1994).

Both global models, Moguntia and HAMOCC3, are not designed to resolve processes within the subgrid coastal regions. Therefore, comparison with measurements is most appropriate in and above the open ocean.

## 2b. MSC-W of EMEP model

The MSC-W model provides estimates of  $\text{NH}_3$  (g) and  $\text{NH}_4^+$  (p) concentrations and depositions arising from emissions in each European country as well as fluxes between each country and to the sea (Tuovinen et al. 1994). The region covered by the model includes the northeast Atlantic, the European Arctic Ocean, and the North, Norwegian, Baltic, Black, and Mediterranean Seas. The model has a single layer Lagrangian formulation representing transport in the European boundary layer. It has a resolution of 150 km at 60° N and calculates mass-balance changes in air parcels traveling on 4-day trajectories to defined receptor points. The model uses actual meteorology which is updated every 6 hours. Wet and dry deposition rates are determined at this frequency. With a resolution of 150 km, the model can not resolve processes in the coastal transition zone but can describe regional sea sub-basins as well as wider oceanic regions.

Nitrogen and sulfur chemistry routines are combined such that ammonia exists as  $\text{NH}_3$  (g) and  $\text{NH}_4^+$  (p) associated with nitrate or sulfate aerosol. Three  $\text{NH}_3$  molecules combine irreversibly with two of  $\text{SO}_4^-$  to form  $(\text{NH}_4)_{1.5}\text{SO}_4$  (assuming that  $(\text{NH}_4)_2\text{SO}_4$  and  $\text{NH}_4\text{HSO}_4$  occur equally) until either no ammonia or no sulfate remains. Remaining ammonia then enters into equilibrium with nitric acid. The nitrate equilibrium point is defined according

to  $K = \text{NH}_{3(\text{eq})} \text{HNO}_{3(\text{eq})}$  with (eq) indicating equilibrium concentrations. If the product of non-equilibrium concentrations is larger than  $K$ ,  $\text{NH}_4\text{NO}_3$  is formed. If the product is smaller,  $\text{NH}_4\text{NO}_3$  dissociates to form its precursor gases. In remote oceanic regions with abundant sulfur present,  $\text{NH}_4\text{NO}_3$  may be of little consequence. Where  $\text{NH}_3$  (g) emissions exceed the sulfur capacity of the aerosol, as with the southern North Sea, 20% of  $\text{NH}_4^+$  (p) may exist as  $\text{NH}_4\text{NO}_3$ . This compares to 4.5% for the entire model domain for this time period.

The model has been modified for this study to estimate the upper limit of the sea-to-land flux of ammonia for European sea areas that border the North Atlantic Ocean by incorporating emissions from the ocean. An air/sea equilibrium between  $\text{NH}_x$  (s) and  $\text{NH}_3$  (g) has been added to the model and is described by Henry's law as given in Section 5a.

### 3. Measured and modeled seawater $\text{NH}_x$ (s) concentrations

#### 3a. *Measured values*

A representative selection of seawater  $\text{NH}_x$  (s) concentrations is listed in Table 2. The colorimetric Berthelot method was used to determine the  $\text{NH}_x$  (s) concentrations in all cases except those reported by Brzezinski (1988) and Lipschultz (this work). Brzezinski (1988) used the Berthelot method followed by solid phase extraction to concentrate the indophenol dye and lower the detection limit. The method used by Lipschultz involves the derivatization of  $\text{NH}_x$  (s) to form a highly fluorescent compound (Jones 1991).

The measurement of  $\text{NH}_x$  (s) is difficult due to contamination during sampling, storage, and analysis (D'Elia 1983). These analytical difficulties become critical at the nanomolar levels of  $\text{NH}_x$  (s) present in most of the world's oceans. The development of new techniques (Brzezinski 1988; Jones 1991) has made a more precise analysis ( $\pm 2$  nM) with a lower detection limit ( $< 10$  nM) possible but an intercomparison of these methods is needed to determine their accuracy. The wide range of values reported for the Sargasso Sea near Bermuda illustrates these analytical difficulties. Concentrations near the detection limit of the colorimetric method, 30 to 50 nM, have been reported for this region (Glibert & McCarthy 1984; Glibert et al. 1988) as well as values as high as 2720 nM (Carpenter 1973). Measurements made with methods which have lower detection limits reveal surface concentrations in the 10 nM range (Brzezinski 1988; Lipschultz, this work). As shown in Figure 1, the only seasonal measurements for this region suggest that values do not exceed 200 nM (Lipschultz, this work) indicating that an average concentration near 50 nM or less is appropriate.

Table 2. Measured  $[\text{NH}_x]_s$  for the North Atlantic.

Site	Date	$[\text{NH}_x]_s$ , nM	Method	Reference
Caribbean 12N, 59W to 17N, 69W	Aug. to Sept., 1977	70–960	Berthelot reaction	Glibert & McCarthy 1984
Caribbean to Bermuda, 23N to 34N, 71W	May	1920–2720	Berthelot reaction	Carpenter 1973
Sargasso Sea	June to July, 1979	<30	Berthelot reaction	Glibert & McCarthy 1984
Sargasso Sea 34N, 73W	May to June, 1982	<30	Berthelot reaction	Glibert et al. 1988
Sargasso Sea 38N, 65W	Sept., 1988	$90 \pm 65$	Berthelot reaction	Longhurst et al. 1989
Sargasso Sea 32N, 62W	June, 1987	10 to 160	Berthelot reaction with solid phase extraction	Brzezinski 1988
Near Bermuda	Sept. to Oct.	60–1070 mean = 460	Berthelot reaction	Carpenter & McCarthy 1975
Bermuda 32N, 64W	Sept. 1992 to April, 1994	10 to 200	OPA derivatization	Lipschultz, this work
SE US Shelf, 32N, 80W	April	300 to 400	Berthelot reaction	Hanson & Robertson 1988
Equator, 0 to 2N, 4W	Various	<50	Berthelot reaction	Le Bouteiller 1986
NW African Coast 31N, 10W to 15N, 18W	March to April, 1971	500 to 1000	Berthelot reaction	Slawyk & MacIsaac 1972
Belgium Coast, 51N, 3E	Spring	600 to 4600	Berthelot reaction	Lancelot et al. 1986

Table 2. Continued.

Site	Date	[NH <sub>x</sub> ] <sub>s</sub> , nM	Method	Reference
Scotian Shelf, 43.5N, 62.5W	Various	500 to 1000	Berthelot reaction	Cochlan 1986
W. Canadian Arctic, 67N, 56W	July	240	Berthelot reaction	Harrison 1983
North Atlantic 40N, 47W 45N, 41W	April to May, 1989	80–300	Berthelot reaction	Harrison et al. 1993
North Atlantic 47N, 20W	May	50	Berthelot reaction	Garside & Garside 1993
North Sea	Feb. to Oct., 1989	300 to 4300	Berthelot reaction	Asman et al. 1994 Brockman et al. 1990

Values reported for the equatorial Atlantic near 4° W also are near the detection limit of the colorimetric technique (<50 nM) (Le Bouteiller 1986). In this southern region, NH<sub>x</sub> (s) concentrations remain low throughout the year as the water column is permanently stratified and the euphotic zone is isolated from the deep water nitrate reservoir. The northern Atlantic Basin, however, experiences a bloom of phytoplankton in the springtime when the water column restratifies after wintertime convection of deep water brings nitrate to the surface. As the bloom ends, decomposition of the increased biomass can lead to higher levels of NH<sub>x</sub> (s) for a short period. This is reflected in the higher concentrations reported for the North Atlantic (up to 300 nM) (Harrison et al. 1993) and the North Sea (up to 4300 nM) (Asman et al. 1994). Reported values also are high in coastal regions including the northwest African coast (500 to 1000 nM) (Slawyk & MacIsaac 1972), the Belgium coast (600 to 4600 nM) (Lancelot et al. 1986), the Scotian Shelf (500 to 1000 nM) (Cochlan 1986), and along the southeastern U.S. (300 to 400 nM) (Hanson & Robertson 1988).

### 3b. Modeled values

Surface NH<sub>x</sub> (s) concentrations calculated from the HAMOCC3 model for the North Atlantic are shown in Figures 2a through 2d for the months of October, January, April, and July, respectively. Annual mean concentrations



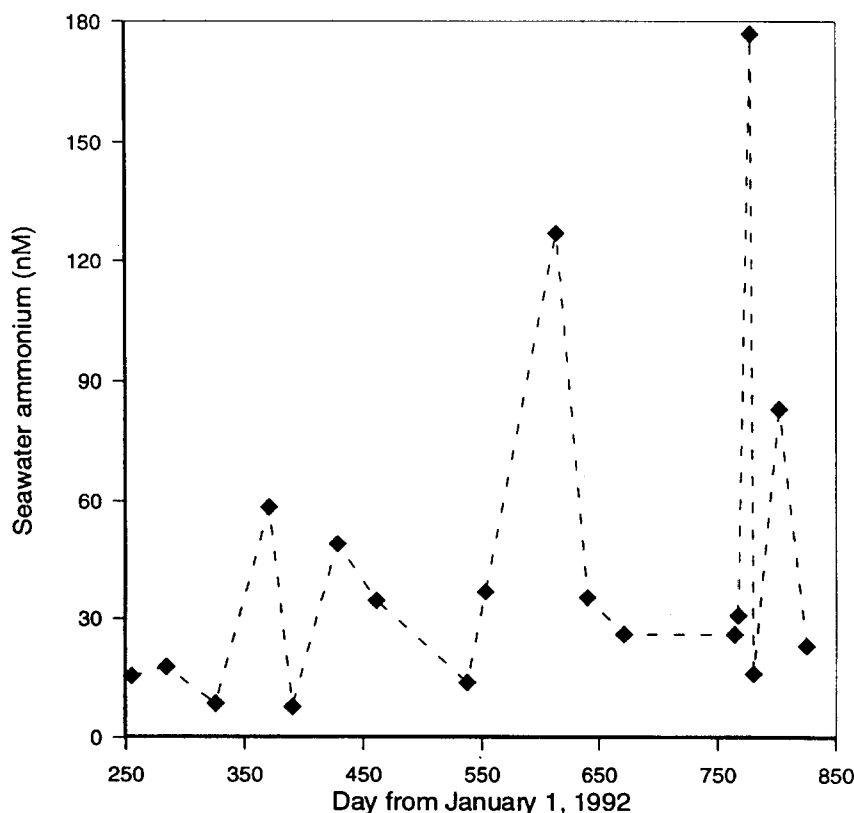
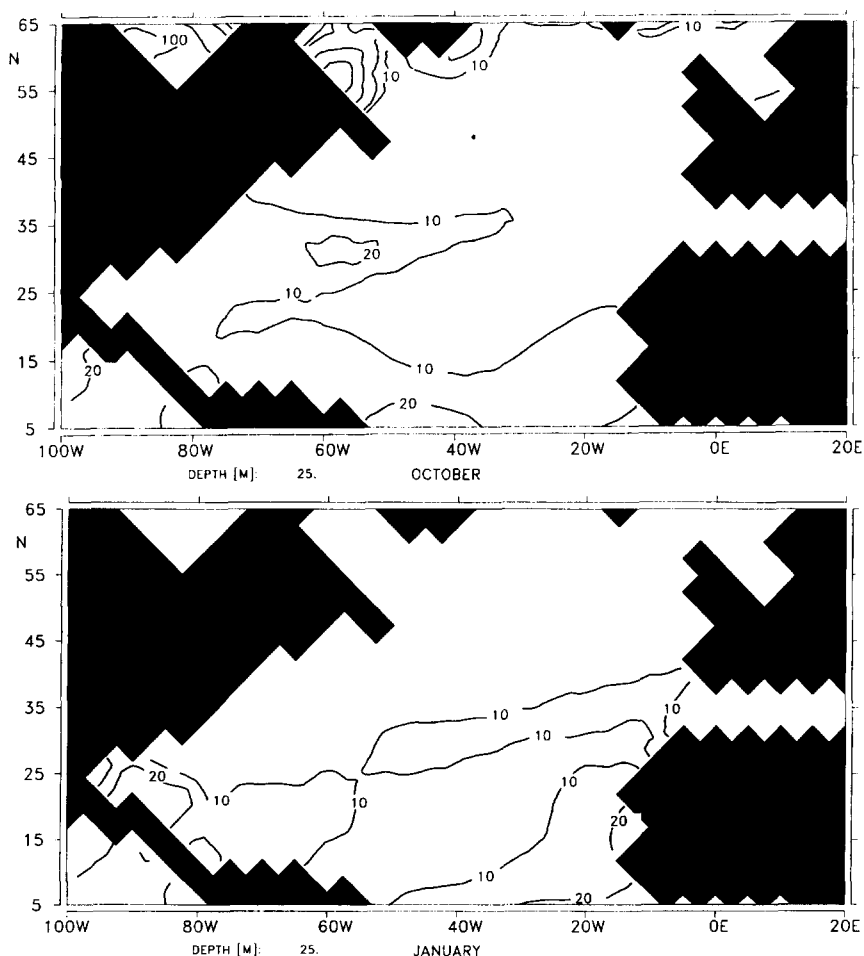


Figure 1. Results of time series measurements of  $\text{NH}_4^+$  (s) concentrations made near Bermuda at  $31.8^\circ \text{ N}$  and  $64.1^\circ \text{ W}$  with the fluorescence technique of Jones (1991). Concentrations are in units of nM.

range from 10 to 50 nM (Figure 2e) with lower values in the subtropical gyres and higher values at latitudes between  $45^\circ$  and  $65^\circ \text{ N}$ . Seasonally, the lowest concentrations occur in fall and winter. Highest concentrations are found during and after plankton blooms; values up to 200 nM occur in the mid-Atlantic at  $30^\circ \text{ N}$  in April and at  $45^\circ$  to  $65^\circ \text{ N}$  in July. Concentrations higher than 200 nM are not predicted for the North Atlantic at latitudes below  $65^\circ \text{ N}$ .

The modeled and measured open ocean  $\text{NH}_4^+$  (s) concentrations fall within the same range; both are  $<30 \text{ nM}$  for the Sargasso Sea and 10 to 100 nM for Bermuda. The model underestimates coastal values by as much as an order of magnitude, however. For example, off the northwestern African coast, values in the range of 500 to 1000 nM have been observed during March and April (Slawyk & McIsaac 1972) but the model values remain between



*Figure 2.* Global distribution of  $\text{NH}_4(\text{s})$  concentrations calculated by the HAMOCC3 model for a) October, b) January, c) April, and d) July. Annually averaged values are shown in e). Concentrations are in units of nM. Isolines are given in logarithmic scaling: 10, 20, 50, 100, and 200 nM.

10 and 20 nM throughout the year. This discrepancy between measured and modeled results in coastal regions can be explained by the coarse resolution of the model. The complex small scale structure of dynamical and biological processes that exist in coastal areas is not well represented by a global ocean model. In addition, year-to-year variability can not be reproduced accurately by HAMOCC3 as it is based on climatological forcing. Hence, the model results will not reflect the change in the measured concentration from 5 to 40 nM near Bermuda in February, 1993 to 180 nM in February, 1994 (Figure 1). The comparison of point measurements with HAMOCC3 values is most

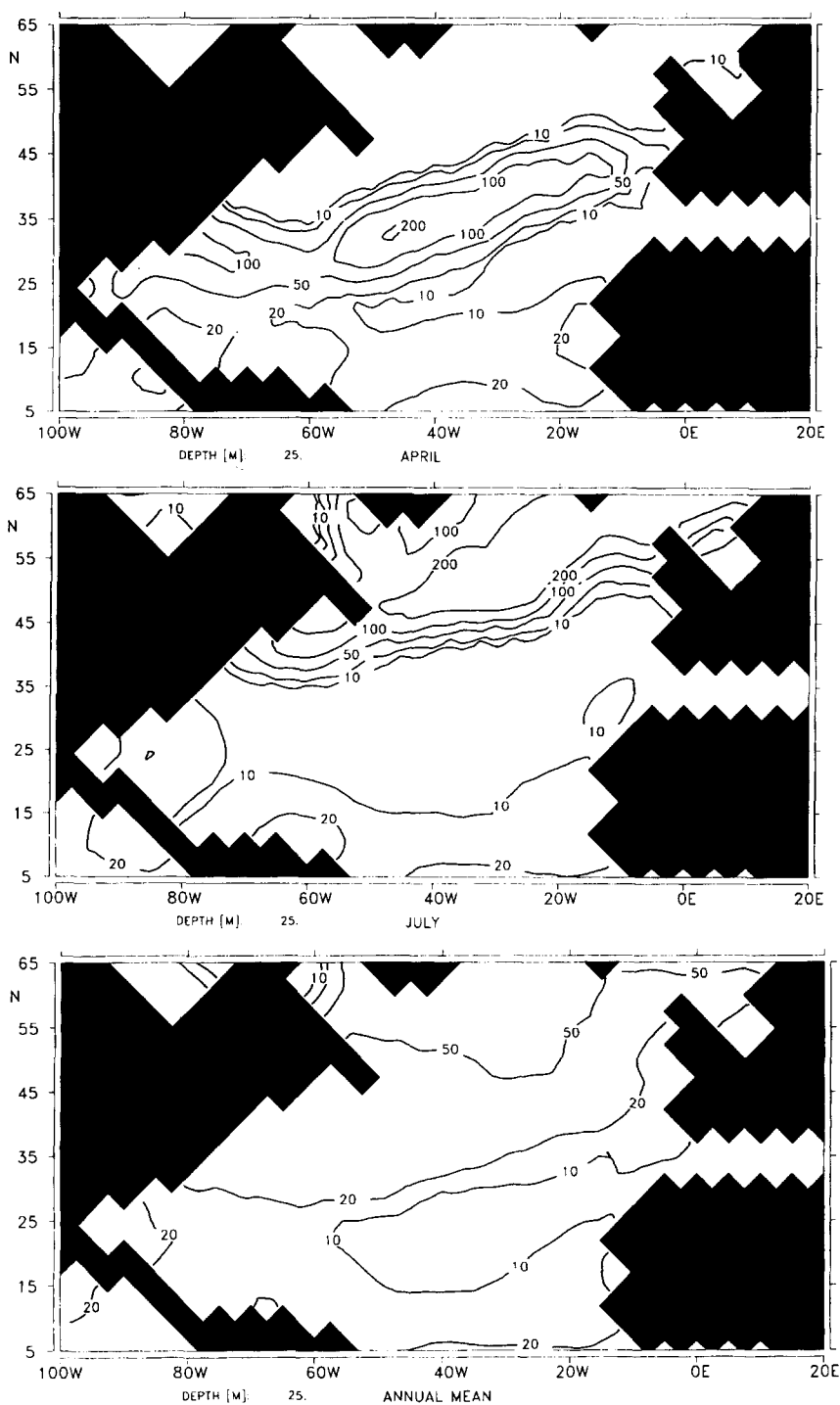


Figure 2. Continued.

appropriate in open ocean regions where spatial and temporal variability is minimized. The agreement within a factor of 2 in large scale structures between observations and HAMOCC3 predictions indicates that the simulated fields can serve as lower ocean boundary conditions for Moguntia.

#### 4. Measured and modeled atmospheric $\text{NH}_3$ (g) concentrations

##### 4a. *Measured values*

Reported values for atmospheric  $\text{NH}_3$  (g) concentrations are listed in Table 3. The data are a result of four field experiments in which different measurement methods and, presumably, different protocols to prevent sample contamination were used. Georgii & Gravenhorst (1977) report results from a cruise taken in October of 1973 that traveled between Hamburg, Germany and the Caribbean Sea. No indication is given of the measurement method or precautions taken to avoid sample contamination. High  $\text{NH}_3$  (g) concentrations were found near the Azores (50 to 170  $\text{nmol m}^{-3}$ ) and over the Caribbean (220  $\text{nmol m}^{-3}$ ) and Sargasso Seas (110 to 500  $\text{nmol m}^{-3}$ ). Lower concentrations of 11 to 60  $\text{nmol m}^{-3}$  were measured over the tropical Atlantic along a transect from 40W to 10W. The high concentrations over the Sargasso Sea prompted the authors to suggest that the ocean was acting as a source of  $\text{NH}_3$  in this region. This can not be confirmed, however, without simultaneously measured  $\text{NH}_x$  (s) concentrations. The high concentrations near the Azores and over the Sargasso Sea contrast with more recent measurements. Zhuang & Huebert (1994) measured concentrations at Santa Maria island in the Azores with annular denuders and found values between 1 and 30  $\text{nmol m}^{-3}$  with an average and standard deviation of  $9 \pm 9.4 \text{ nmol m}^{-3}$ . LeBel et al. (1985) measured concentrations at Bermuda of 20  $\text{nmol m}^{-3}$  using the  $\text{WO}_x$  denuder technique. It is unclear if these large discrepancies are a result of sampling artifacts or natural variability.

More recently, Asman et al. (1994) reported concentrations of 2 to 140  $\text{nmol m}^{-3}$  for the North Sea using  $\text{H}_3\text{PO}_4$  impregnated filters. This is the only experiment of the four in which simultaneously measured  $\text{NH}_x$  (s) concentrations were reported.

##### 4b. *Modeled values*

$\text{NH}_3$  (g) concentrations for the months of October, January, April, and July calculated with the Moguntia model are shown in Figures 3a through 3d, respectively. Annually averaged values are shown in Figure 3e. In the fall and winter, concentrations are low throughout the open ocean of the North

Table 3. Measured atmospheric  $\text{NH}_3$  (g) concentrations,  $(\text{NH}_3)_g$ , for the North Atlantic Basin.

Site	Date	$(\text{NH}_3)_g$ , $\text{nmol m}^{-3}$	Method	Reference
North Sea South of 56N	March to Sept., 1989	2–140	Impregnated $\text{H}_3\text{PO}_4$ filter	Asman et al. 1994
North Sea, English Channel	October, 1973	42–180	Not given	Georgii & Gravenhorst 1977
Azores 30N to 40N	October, 1973	50–170	Not given	Georgii & Gravenhorst 1977
Azores 37N, 25W	June, 1992	1–30	Denuder	Zhuang & Huebert 1994
Tropical Atlantic 40W to 10W	October, 1973	11–60	Not given	Georgii & Gravenhorst 1977
Caribbean 70W	October, 1973	220	Not given	Georgii & Gravenhorst 1977
Sargasso Sea 20N to 30N	October, 1973	110–500	Not given	Georgii & Gravenhorst 1977
Bermuda	1982	20	$\text{WO}_3$ Denuder	LeBel et al. 1985

Atlantic; values are around  $1.0 \text{ nmol m}^{-3}$  at  $30^\circ \text{ N}$  and increase to 5 to  $10 \text{ nmol m}^{-3}$  over the Sargasso Sea and between  $5^\circ$  and  $15^\circ \text{ N}$ . Concentrations are higher over the Gulf of Mexico ( $5$  to  $10 \text{ nmol m}^{-3}$ ), Caribbean Sea ( $10$  to  $20 \text{ nmol m}^{-3}$ ), and North Sea ( $2$  to  $10 \text{ nmol m}^{-3}$ ). Along the coasts of Ireland, France, and Portugal, concentrations range from  $2$  to  $10 \text{ nmol m}^{-3}$ . During the summer, concentrations increase to  $5 \text{ nmol m}^{-3}$  over the North Atlantic but decrease to  $0.5 \text{ nmol m}^{-3}$  further south near  $25^\circ \text{ N}$ . Summer concentrations are similar to those calculated for the winter months over the Gulf of Mexico, the Sargasso Sea and the Caribbean Sea. They are higher, however, over the North Sea and the coasts of Ireland, France, and Portugal reaching values of  $20 \text{ nmol m}^{-3}$ .

Annually averaged  $\text{NH}_3$  (g) concentrations calculated with the MSC-W model for the year 1990 are shown in Figure 4. These calculations use a polynomial interpolation between grid squares. The values are based on  $\text{NH}_3$  emissions resulting from agricultural and industrial activity and, hence, are of purely anthropogenic origin. Over the open ocean,  $\text{NH}_3$  (g) concentrations

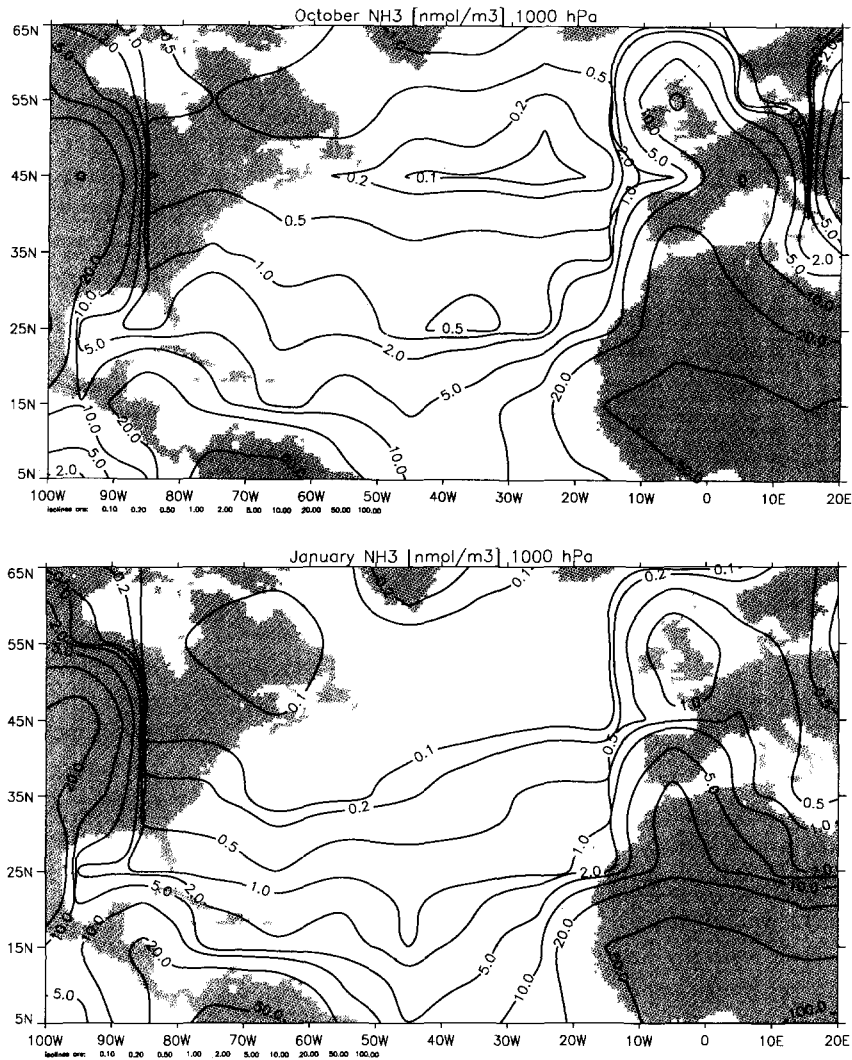
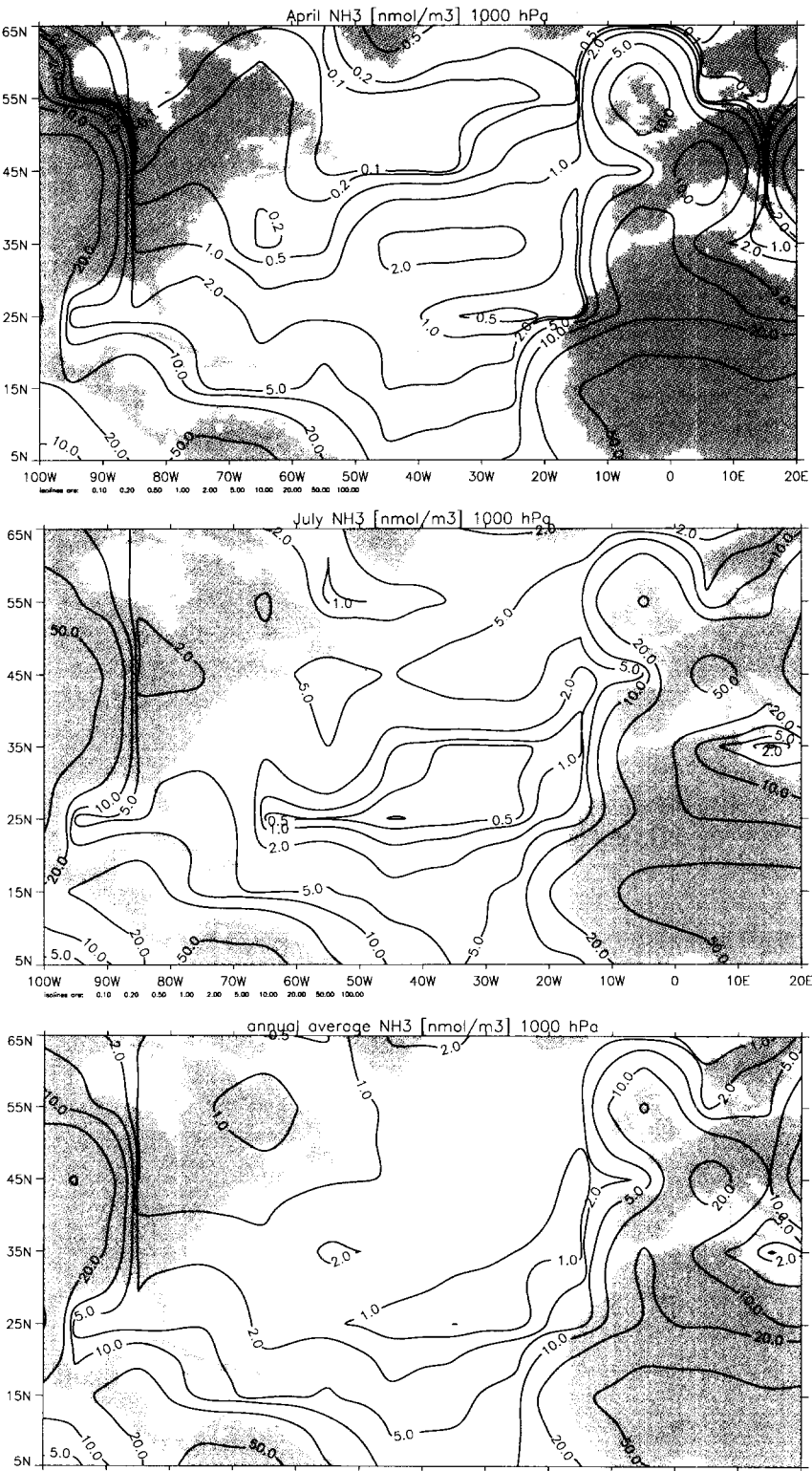


Figure 3. Global distribution of  $\text{NH}_3$  (g) calculated by Moguntia for a) October, b) January, c) April, and d) July. Annually averaged values are shown in e). Concentrations are in units of  $\text{nmol m}^{-3}$ .

are below  $2 \text{ nmol m}^{-3}$ . Over the North Sea, concentrations range from 2 to  $100 \text{ nmol m}^{-3}$  with values decreasing northwards. Along the coast of Ireland, gradients are steep with concentrations on land being over  $50 \text{ nmol m}^{-3}$  and those 150 km from the coast being below  $2 \text{ nmol m}^{-3}$ . Adjacent to the coasts of France and Portugal they are over  $50 \text{ nmol m}^{-3}$ . Throughout this region, concentrations decrease with distance from the shore.



# Estimated $\text{NH}_3$ concentrations, year 1990 from terrestrial anthropogenic sources

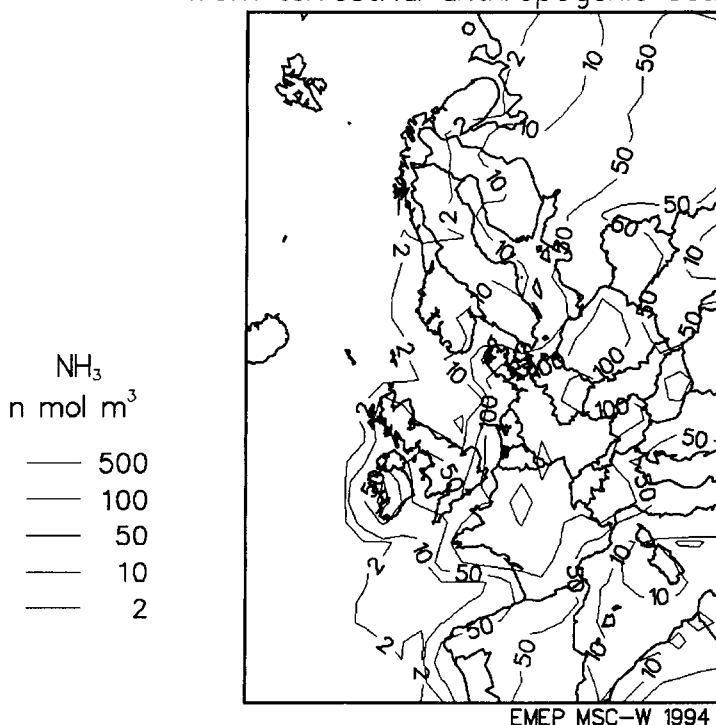


Figure 4. Annually averaged distribution of atmospheric  $\text{NH}_3$  (g) for the northeast Atlantic Basin calculated from the MSC-W model for the year 1990. Concentrations are in  $\text{nmol m}^{-3}$ .

The two models predict similar annually averaged values for the North Sea (Moguntia: 2 to 10 and MSC-W: 2 to over  $100 \text{ nmol m}^{-3}$ ) and the NE Atlantic (Moguntia: 1 to 5 and MSC-W: below  $2 \text{ nmol m}^{-3}$ ). As expected, however, this level of agreement does not extend to regions over land where large point sources can exist. This lack of agreement is due to differences in the model characteristics. MSC-W has a resolution of 150 km. The resolution of Moguntia is 1000 km which leads to a dilution of sources and a lowering of the calculated  $\text{NH}_3$  (g) concentrations. Transport schemes also are different as MSC-W uses actual meteorology and Moguntia uses monthly averaged winds. In addition, emissions from MSC-W are more specific in location than those from Moguntia.

In all regions where both measured and modeled concentrations of  $\text{NH}_3$  are available, the measured values are about an order of magnitude larger. One exception is over the North Sea where modeled values are within the range



of those that were measured. The systematically higher measured values may be a result of contamination during sample collection and analysis in areas with low concentrations. Additionally, the models could be underestimating the emissions of  $\text{NH}_3$  (g) or overestimating the fraction of  $\text{NH}_3$  (g) that is converted to  $\text{NH}_4^+$  (p). The latter seems unlikely considering the fast reaction rate between  $\text{NH}_3$  (g) and sulfate aerosol (Quinn et al. 1992). A final difficulty is that continental modeling at scales in excess of 100 km resolution can not resolve sharp concentration gradients. Hence, for regions with large  $\text{NH}_3$  sources, values derived from point measurements are expected to differ from those derived from wider-scale models.

## 5. Air/sea $\text{NH}_3$ fluxes

### 5a. Description of flux calculation

The following method (Asman et al. 1994) was used to calculate the air/sea  $\text{NH}_3$  flux from the measured concentrations of  $\text{NH}_3$  (g) and  $\text{NH}_x$  (s). The same method is used in the MSC-W model and the Moguntia/HAMOCC3 models. The flux of ammonia across the air/sea interface is parameterized as the product of the exchange velocity,  $V_e$ , and the difference between the concentration of ammonia in equilibrium with dissolved ammonia in the sea surface,  $\text{NH}_3$  (s,eq), and the concentration of atmospheric ammonia,  $\text{NH}_3$  (g), such that

$$F = V_e[(\text{NH}_3)_{\text{s,eq}} - (\text{NH}_3)_g] \quad (1)$$

For flux estimates derived from measured concentrations, a constant exchange velocity of  $0.8 \text{ cm s}^{-1}$  was used. This exchange velocity is based on experimentally determined transfer rates of water at air/water interfaces (Liss & Galloway 1993) recognizing that  $\text{NH}_3$  and  $\text{H}_2\text{O}$  have similar molecular structures and behaviors. Values of  $V_e$  used in the MSC-W model are determined at 6 hour intervals and vary with wind speed and stability assuming no explicit surface resistance to transfer (Tuovinen et al. 1994). Values of  $V_e$  used in the Moguntia/HAMOCC3 models vary with observed wind speeds and range from  $0.8$  to  $2 \text{ cm s}^{-1}$ .

Values of  $(\text{NH}_3)_{\text{s,eq}}$  are derived from

$$(\text{NH}_3)_{\text{s,eq}} = \frac{M_{\text{NH}_3}[\text{NH}_x]_s}{RTH_{\text{NH}_3} \left( \frac{1}{\alpha} + \frac{10^{-\text{pH}}}{\beta K_{\text{NH}_4}} \right)} \quad (2)$$

which takes into account the equilibrium in seawater between  $\text{NH}_3$  (s) and  $\text{NH}_4^+$  (s) and the Henry's law equilibrium between  $\text{NH}_3$  (s) and  $\text{NH}_3$  (s,eq).

Here,  $M_{\text{NH}_3}$  is the molecular weight of  $\text{NH}_3$  ( $17 \text{ g mol}^{-1}$ ),  $[\text{NH}_x]_s$  is the seawater  $\text{NH}_x$  concentration in  $\mu\text{mol l}^{-1}$ ,  $R$  is the gas constant ( $8.2075 \times 10^{-5} \text{ atm m}^3 \text{ mol}^{-1} \text{ K}^{-1}$ ), and  $T$  is temperature in K.  $H_{\text{NH}_3}$  is the Henry's law constant for  $\text{NH}_3$  in  $\text{mol l}^{-1} \text{ atm}^{-1}$  and is given by

$$H_{\text{NH}_3} = 56 \exp \left( 4092 \left( \frac{1}{T} - \frac{1}{298.15} \right) \right) \quad (3)$$

(Dasgupta & Dong 1986).  $\alpha$  is the activity coefficient of  $\text{NH}_3$  (s) and is given by

$$\alpha = 1 + 0.085I \quad (4)$$

(Garrels & Christ 1965) where  $I$  is the seawater ionic strength such that

$$I = 0.00147 + 0.01988S + 2.08357 \times 10^{-5}S^2 \quad (5)$$

and  $S$  is salinity (Lyman & Fleming 1940). The activity coefficient of  $\text{NH}_4^+$  is  $\beta$  where

$$\beta = 10^\gamma \quad (6)$$

(Seinfeld 1986) and

$$\gamma = -A_i z (\sqrt{I} / (1 + \sqrt{I}) - 0.2I) \quad (7)$$

Here,  $A_i = A + BT + CT^2$ ,  $A = 0.4896844$ ,  $B = -0.0007477$ ,  $C = 2.729 \times 10^{-6}$ , and  $z$  is the charge on the ion. The dissociation constant of  $\text{NH}_4^+$  is in units of  $\text{mol l}^{-1}$  and is given by

$$K_{\text{NH}_4} = 5.67 \times 10^{-10} \exp \left( -6286 \left( \frac{1}{T} - \frac{1}{298.15} \right) \right) \quad (8)$$

(Bates & Pinching 1950).

#### 5b. Flux estimates derived from measured concentrations

Reported concentrations of atmospheric  $\text{NH}_3$  (g) and seawater  $\text{NH}_x$  (s) were used to calculate fluxes for those regions of the North Atlantic where both atmospheric and seawater data are available. These regions include the Caribbean and Sargasso Seas, Bermuda, and the North Sea. The measurements from the North Sea are the only ones in which the atmospheric and oceanic data were collected simultaneously. For the other regions, the

atmospheric and seawater data were collected at different times by different researchers. Samples for atmospheric  $\text{NH}_3$  (g) are collected for longer periods of time than are samples for  $\text{NH}_x$  (s) and will be representative of a larger region. The seawater samples may be collected at a depth that does not represent the surface layer concentration that determines the flux. As a result, the flux estimates reported here are intended to be a first approximation for the North Atlantic Ocean. As these estimates are derived from discrete measurements, they are "point-in-time" fluxes and are not time averaged net balances of deposition and emission.

Estimated fluxes as well as the input parameters for the calculation are shown in Table 4. A uniform surface seawater pH of 8.1 was assumed and annually averaged sea surface temperatures (Pickard & Emery 1982) and salinities (Taylor & Stevens 1980) were used. For the Caribbean Sea, a fixed atmospheric  $\text{NH}_3$  (g) concentration but a varying seawater concentration was used which resulted in flux values ranging from  $-150$  to  $-110 \mu\text{mol m}^{-2} \text{d}^{-1}$ . The low concentrations of  $\text{NH}_x$  (s) resulted in a flux from the atmosphere to the ocean.

Two sets of flux calculations were performed for the region of the Sargasso Sea. In the first, measured  $\text{NH}_x$  (s) and  $\text{NH}_3$  (g) concentrations from the wider region of the Sargasso Sea were used so that  $\text{NH}_x$  (s) ranged between 10 and 160 nM (Brzezinski 1988) and the  $\text{NH}_3$  (g) ranged from 110 to 500 nmol  $\text{m}^{-3}$  (Georgii & Gravenhorst 1977). The large measured concentrations of atmospheric  $\text{NH}_3$  led to a consistent flux from the atmosphere to the ocean ranging between  $-340$  and  $-6 \mu\text{mol m}^{-2} \text{d}^{-1}$ . In the second estimation, data taken near and on Bermuda were used. A range of  $\text{NH}_x$  (s) concentrations from 10 to 200 nM (Lipschultz, this work) and an average  $\text{NH}_3$  (g) concentration of 20 nmol  $\text{m}^{-3}$  (LeBel 1985) resulted in an estimated flux of  $-13$  to  $-5.8 \mu\text{mol m}^{-2} \text{d}^{-1}$ . The discrepancy between these two calculated fluxes for the Sargasso Sea results from a large difference in the measured  $\text{NH}_3$  (g) concentrations. It is likely that the early measurements of Georgii & Gravenhorst (1977) suffered from artifacts or contamination during sampling that led to artificially high concentrations. This is supported by the factor of ten difference in the concentrations measured in the Azores by Zhuang & Huebert (1994) (1 to 30 nmol  $\text{m}^{-3}$ ) and Georgii & Gravenhorst (1977) (50 to 170 nmol  $\text{m}^{-3}$ ). This assumption of an artifact in the Georgii & Gravenhorst (1977) measurements can not be confirmed, however, as no indication of the technique used or precautions that were taken to prevent contamination is given.

For the North Sea, where seawater and atmospheric concentrations were measured simultaneously (Asman et al. 1994), flux estimates vary from  $-75$  to  $43 \mu\text{mol m}^{-2} \text{d}^{-1}$ . The net direction of the flux appears to be determined

Table 4.  $\text{NH}_3$  flux estimates based on measured  $(\text{NH}_3)_g$  and  $[\text{NH}_x]_s$  and the Moguntia/HAMOCC3 and MSC-W models.  $[\text{NH}_x]_s$  are in units of nM,  $(\text{NH}_3)_g$  are in  $\text{nmol m}^{-3}$ , and fluxes are in  $\mu\text{mol m}^{-2} \text{d}^{-1}$ .

Region	$[\text{NH}_4]_s$ Measured	$[\text{NH}_4]_s$ MOG	$[\text{NH}_4]_s$ MSC-W	$(\text{NH}_3)_g$ Measured	$(\text{NH}_3)_g$ MOG	$(\text{NH}_3)_g$ MSC-W	Flux Measured	Flux MOG <sup>a</sup>	Flux MSC-W <sup>b</sup>
Caribbean	70–960 <sup>1</sup>	20–60	220 <sup>5</sup>	3–25			–150 to –110	–4.0 to 1.3	
Sargasso	10–160 <sup>2</sup>	10–180	110–500 <sup>5</sup>	4–10			–340 to –76		
Bermuda	10–200 <sup>3</sup>	10–100	20 <sup>6</sup>	2–5			–13 to –5.8	4.0	
North Sea	300–4300 <sup>4</sup>	10–270	1000	1–20	2–100		–75 to 43 <sup>4</sup>	–1.3 to 1.3	–69 to 20
NE Atlantic 40N, 12W		10–250	250	1–3	2–50			0 to 1.3	–1.6 to 3.3
NE Atlantic 50N, 20W		10–250	250	5	0.1			1.3 to 2.7	1.3
Coast of Ireland		10–280	250	1–25	2–10			–1.3 to 0	1.4
Coast of France & Portugal		10–140	250	3–25	2–50			0 to 1.3	–1.6 to 3.3

<sup>a</sup> Net monthly average flux, <sup>b</sup> Disaggregated fluxes

<sup>1</sup> Glibert & McCarthy (1984), <sup>2</sup> Brzezinski (1988), <sup>3</sup> This work, <sup>4</sup> Asman et al. (1994), <sup>5</sup> Georgii & Gravenhorst (1977), <sup>6</sup> Lebel et al. (1985)

by the highly variable  $\text{NH}_3$  (g) concentration which, in turn, is a result of the proximity of the measurements to continental source regions. Lower  $\text{NH}_3$  (g) concentrations in mid-summer yield near zero fluxes while higher values at other times of the year lead to atmosphere-to-ocean fluxes.

### 5c. Flux estimates derived from modeled values

Flux estimates from the Moguntia and MSC-W models are compared to those derived from the measured concentrations in Table 4. Net fluxes were derived from the Moguntia/HAMOCC3 models using HAMOCC3 calculated  $\text{NH}_x$  (s) concentrations, sea surface temperature, and pH and Moguntia calculated  $\text{NH}_3$  (g). Fluxes from gridboxes partly covered by the ocean were scaled using the oceanic areal fraction. Calculated fluxes for the Caribbean Sea ranged from  $-4.0$  to  $1.3 \mu\text{mol m}^{-2} \text{d}^{-1}$ . Around Bermuda, the flux consistently was from the ocean to the atmosphere with a value near  $4.0 \mu\text{mol m}^{-2} \text{d}^{-1}$ . Over the northeast Atlantic, fluxes were positive and were between  $0$  and  $1.3 \mu\text{mol m}^{-2} \text{d}^{-1}$  at  $40^\circ \text{N}$  and  $12^\circ \text{W}$  and  $1.3$  and  $2.7 \mu\text{mol m}^{-2} \text{d}^{-1}$  at  $50^\circ \text{N}$  and  $20^\circ \text{W}$ . Fluxes from the North Sea were both slightly negative and slightly positive such that, on the average, they were near zero. Near the coasts of Ireland and France, fluxes were both negative and positive with values of  $-1.3$  to  $0$  and  $0$  to  $1.3 \mu\text{mol m}^{-2} \text{d}^{-1}$ , respectively. Over the open ocean, fluxes were on the order of  $1$  to  $2 \mu\text{mol m}^{-2} \text{d}^{-1}$ . These agree well with the lower range of previously reported flux estimates for the central Pacific Ocean (Quinn et al. 1990).

For the flux estimates derived from the MSC-W model, reported seawater concentrations during periods of plankton blooms were used in order to estimate potential maximum fluxes. These concentrations included North Sea values of  $1000$  to  $4000 \text{ nM}$  (Brockman et al. 1990; Asman et al. 1994) and North Atlantic values of  $250 \text{ nM}$  (Harrison et al. 1993). All coastal waters (mixed land/sea grid squares) were given a concentration of  $500 \text{ nM}$ . Sea surface temperatures were obtained from the Numerical Weather Prediction (NWP) model of the Norwegian Meteorological Institute. Input salinity values for the northeast Atlantic and North Sea were  $35$  and  $34$  per mil, respectively (Taylor & Stevens 1980). A surface seawater pH of  $8.1$  was assumed for all regions. Using these input values, both net fluxes and disaggregated fluxes, i.e., fluxes separated into the upward and downward direction, were estimated for the month of August 1990. The upward flux of oceanic  $\text{NH}_3$  is shown in Figure 5a. Emissions ranged from  $1.0$  to  $20 \mu\text{mol m}^{-2} \text{d}^{-1}$  for the North Sea. These are comparable with the summertime values derived from measurements of Asman et al. (1994). For the same month, deposition fluxes between  $-0.70$  and  $-69 \mu\text{mol m}^{-2} \text{d}^{-1}$  were estimated (Figure 5b). In both cases, the fluxes decrease from the south to the north. The net flux is smaller than the

disaggregated fluxes, ranging between  $-1.03$  to  $13 \mu\text{mol m}^{-2} \text{d}^{-1}$ , and is a result of the reversals in direction during the course of the month. Over the northeast Atlantic, both emission and deposition fluxes are much smaller than those over the North Sea. Off the coasts of Ireland and France, emission values were  $1.4$  and  $3.3 \mu\text{mol m}^{-2} \text{d}^{-1}$ , respectively ( $1.3$  and  $1.7 \mu\text{mol m}^{-2} \text{d}^{-1}$  net). These are only slightly higher than in the mid North Atlantic at distances of  $1000 \text{ km}$  from the continent where values range from  $1.3$  to  $2.1 \mu\text{mol m}^{-2} \text{d}^{-1}$  with no deposition flux.

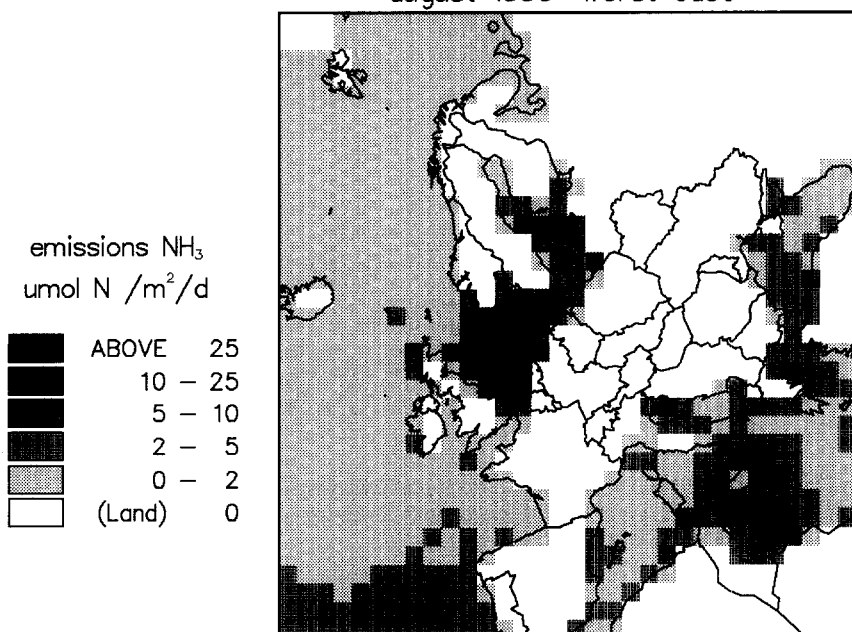
Results from the MSC-W model allow for an assessment of the importance of marine ammonia sources to each European country relative to agricultural and industrial sources. These preliminary calculations, assuming summertime conditions, indicate that marine emissions may be one of the larger external sources of deposited reduced nitrogen for some countries on the western margins of the continent. For Ireland, marine emissions are the second largest source of reduced nitrogen, for the United Kingdom they are the third, for Norway the fifth, and for Finland the sixth. The inclusion of a marine source of reduced nitrogen for the European domain as a whole, however, only increases total emissions by  $1.5\%$ . Winter emission fluxes would be much lower due to colder temperatures and smaller seawater  $\text{NH}_x$  (s) concentrations.

When comparing fluxes from the Moguntia/HAMOCC3 and MSC-W models, net fluxes versus disaggregated fluxes are involved. Yet, in general, the direction of the fluxes predicted by the two models is the same and the magnitudes fall within the same range (Table 4). Flux estimates derived from the measured data are larger in both the negative and positive direction than the model derived values. It is unclear whether this discrepancy is due to inaccurate chemistry and transport schemes in the models, sampling artifacts in the measurements, or factors that make a direct comparison of the measurement- and model-derived results difficult. The measurement-derived fluxes are discrete in time while the model estimates are time averaged. A first step in resolving the disagreement would be to make accurate, simultaneous measurements of  $(\text{NH}_3)_g$  and  $[\text{NH}_x]_s$  and then to compare these to the model derived values over equivalent time periods. Such measurements should be made in several regions of the North Atlantic that have different sea surface temperatures and  $\text{NH}_x$  (s) concentrations as well as atmospheric  $\text{NH}_3$  (g) concentrations. Representative regions with large surface areas such as  $0$  to  $20^\circ \text{ N}$  or the Sargasso Sea would be most relevant for a basin scale assessment.

#### 5d. *Model geography of oceanic $\text{NH}_3$ (g) emission versus deposition*

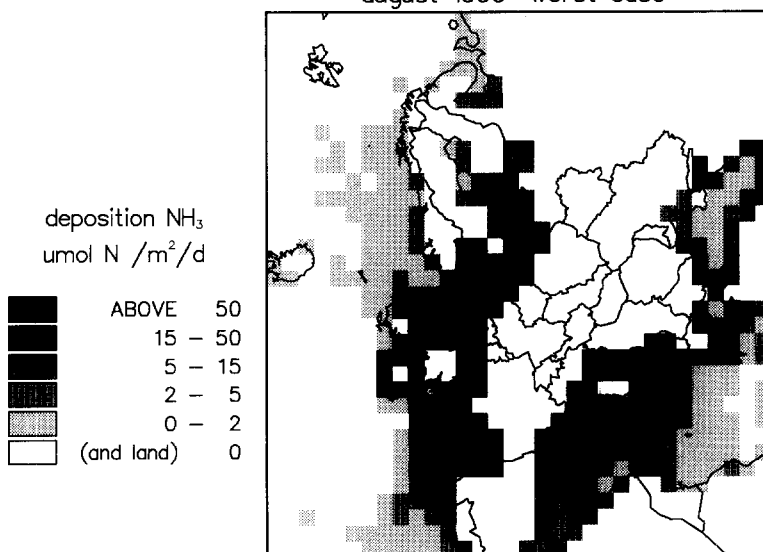
To determine the regions of the North Atlantic that serve as a source of atmospheric  $\text{NH}_3$ , annually averaged net emissions and depositions of  $\text{NH}_3$

### Emission strengths of marine $\text{NH}_3$ august 1990 "worst case"



EMEP MSC-W 1994

### Deposition strengths of $\text{NH}_3$ to marine waters august 1990 "worst case"



EMEP MSC-W 1994

Figure 5. Disaggregated fluxes of ammonia in the a) upward (emission) direction and b) downward (deposition) direction calculated by the MSC-W model for August, 1990. Fluxes are in units of  $\mu\text{mol m}^{-2} \text{d}^{-1}$ .

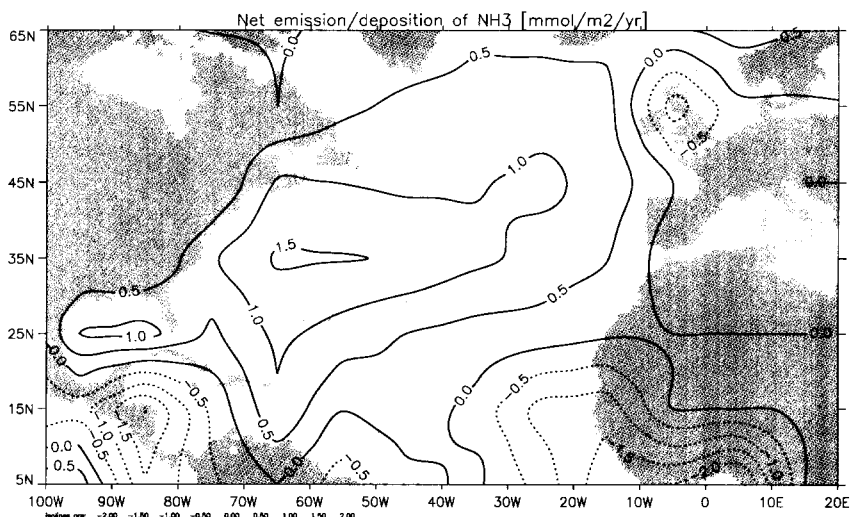


**Figure 6.** Net annually averaged oceanic ammonia emissions (continuous lines) and depositions (dashed lines) calculated with the Moguntia/HAMOCC3 global models. Fluxes are in  $\text{mmol m}^{-2} \text{yr}^{-1}$  ( $1 \text{ mmol m}^{-2} \text{yr}^{-1} = 2.7 \mu\text{mol m}^{-2} \text{d}^{-1}$ ).

from and to the ocean surface were calculated with the Moguntia/HAMOCC3 global models (Figure 6). Emissions and depositions over continental areas, which are an order of magnitude larger than those in oceanic regions, are not shown in this figure. Net  $\text{NH}_3$  deposition occurs in ocean areas that are downwind of continental source regions such as Central America and eastern Africa. In these continentally-derived air masses, the model calculations indicate that ammonia emissions frequently dominate sulfur emissions. Therefore, gas phase  $\text{NH}_3$  does not react immediately with acidic sulfate aerosol so that atmospheric residence times are long enough to allow transport to the oceans. Relatively small net fluxes are calculated over the North Sea due to the magnitude of the upward and downward disaggregated fluxes. The presence of significant  $\text{NH}_x$  (s) concentrations gives rise to large but temporary emission fluxes which are balanced by deposition due to high atmospheric concentrations at other times. The net flux results from the MSC-W model (Figure 7) also suggest a zoning in emission versus deposition during the month considered (August 1990). While the oceanic waters have a uniform emission characteristic, deposition is often dominant in coastal regions that are under the influence of terrestrial sources such as the French coast and the European shelf. Where localized marine concentrations are sufficient, however, net emission can occur such as for the central North Sea.



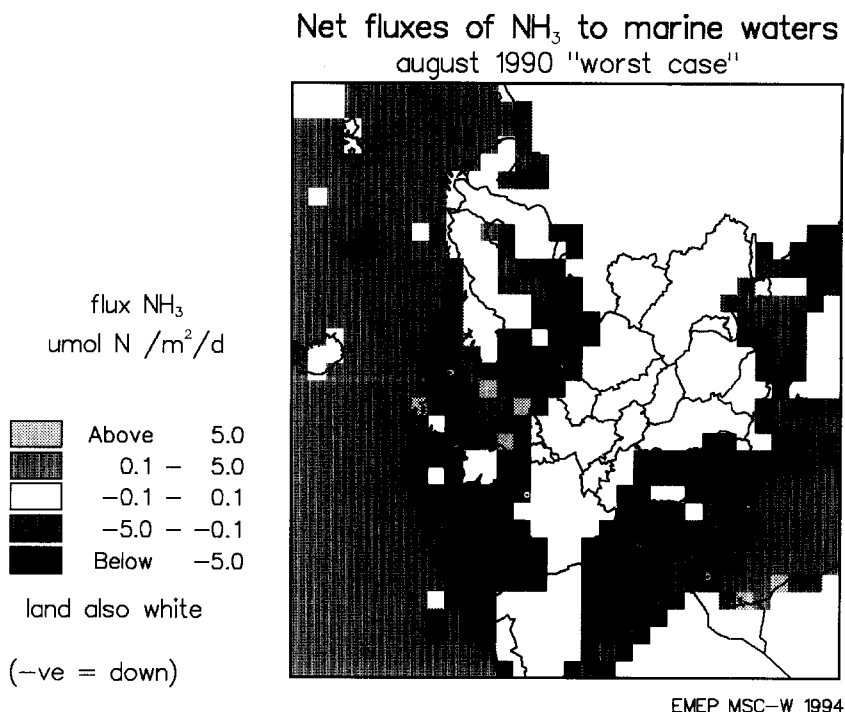


Figure 7. Net fluxes of ammonia for the northeast Atlantic Basin for August 1990 as calculated by the MSC-W model. Fluxes are in units of  $\mu\text{mol m}^{-2} \text{d}^{-1}$ .

## 6. Sensitivity of the flux calculation to input parameters

A sensitivity study was done to quantify the effect that changes in surface seawater temperature, salinity, pH,  $\text{NH}_x$  (s) concentration, the atmospheric  $\text{NH}_3$  (g) concentration, and  $V_e$  have on the calculated flux. The input parameters for the sensitivity calculations were set for a base case of surface seawater temperature equal to 19 °C, salinity equal to 35.75 per mil, pH equal to 8.2,  $[\text{NH}_x]_s$  equal to 100 nM,  $(\text{NH}_3)_g$  equal to 1  $\text{nmol m}^{-3}$ , and  $V_e$  equal to 0.8  $\text{cm sec}^{-1}$ . One parameter was varied at a time while the others were kept at the base case values. Input parameters were varied over the range of values expected for the North Atlantic Basin: temperature from 7 to 31 °C, salinity from 34 to 37.5 per mil, pH from 7.8 to 8.5,  $[\text{NH}_x]_s$  from 10 to 5000 nM,  $(\text{NH}_3)_g$  from 1 to 500  $\text{nmol m}^{-3}$ , and  $V_e$  from 0.8 to 2.0  $\text{cm sec}^{-1}$ . As shown in Figure 8, for the range of expected values of the input parameters, changes in  $[\text{NH}_x]_s$  and  $(\text{NH}_3)_g$  have the largest effect on the absolute magnitude of the flux. Changes in seawater temperature also have a significant effect while changes in salinity, seawater pH, and  $V_e$  have minimal effects.

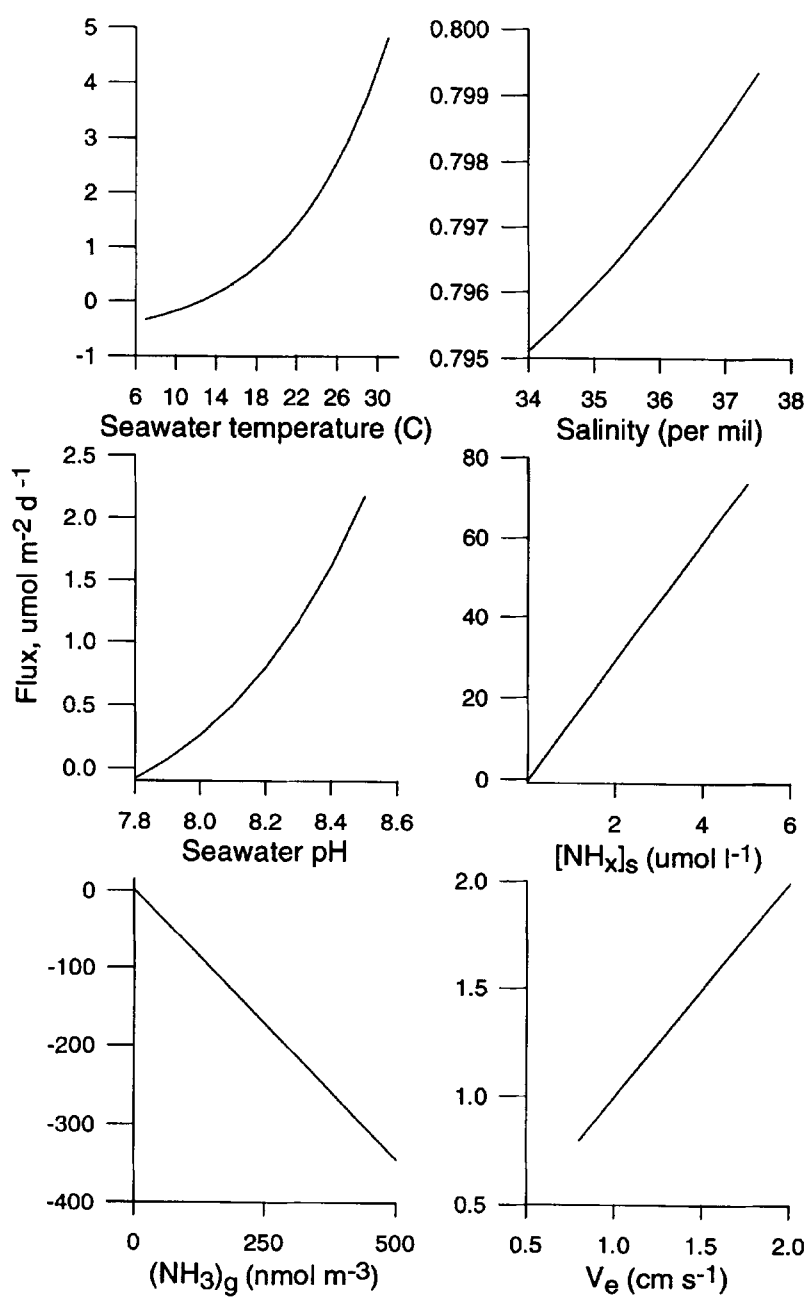


Figure 8. The sensitivity of the calculated flux to changes in surface seawater temperature, salinity, pH,  $[\text{NH}_x]_s$ , atmospheric  $(\text{NH}_3)_g$ , and the exchange velocity,  $V_e$ .

## 7. Conclusions

Presented here is a first attempt to determine the direction and magnitude of the air/sea ammonia flux for different regions of the North Atlantic Basin. Reported seawater and atmospheric ammonia concentrations have been compiled and the measured data have been compared to Moguntia/HAMOCC3 and MSC-W model output. In addition, air/sea  $\text{NH}_3$  fluxes have been derived from the measured and modeled seawater and atmospheric concentration data.

Measured seawater  $\text{NH}_x$  (s) concentrations cover two orders of magnitude ranging from less than 30 to 4300 nM. The highest concentrations are reported for the Caribbean Sea, North Sea, and the Belgium coast. Very few open ocean values have been reported. The HAMOCC3 global model was able to reproduce the measured open ocean concentrations but tended to underestimate coastal values. This most likely is a result of the large scale of the model and an incomplete description within the model of the biological processes controlling the seawater ammonia concentrations. Measured atmospheric  $\text{NH}_3$  (g) concentrations have been reported for only four North Atlantic field experiments. The concentrations range from 2 to 500 nmol m<sup>-3</sup> with the largest values reported for the North Sea, the Caribbean Sea, and the Sargasso Sea. Again, there is a lack of open ocean measurements. In general, measured  $\text{NH}_3$  (g) concentrations were larger than those calculated from the MSC-W and Moguntia models. The systematically higher measured values could be due to sample contamination and/or inadequate emission and transport schemes in the models. In addition, Moguntia concentrations are representative of the lowest 0 to 400 m of the atmosphere while the measurements are made at the surface. The difficulty in comparing point measurements with wider-scale models may also contribute to the disagreement.

Air/sea fluxes of ammonia calculated from the measured seawater  $\text{NH}_x$  (s) and atmospheric  $\text{NH}_3$  (g) concentrations are meant to be a first approximation as, in most cases, the seawater and atmospheric concentrations were not measured simultaneously. The North Sea was found to have both atmosphere-to-ocean and ocean-to-atmosphere net fluxes. Fluxes for the Caribbean, Bermuda, and the Sargasso Sea were consistently from the atmosphere to the ocean although those from the Sargasso Sea were about a factor of 15 to 20 larger than those from Bermuda. The lack of agreement between the Bermuda and Sargasso Sea fluxes is disturbing as they are in the same region. It is likely that the  $\text{NH}_3$  (g) concentrations measured over the Sargasso Sea (Georgii & Gravenhorst 1977) were contaminated leading to artificially large atmosphere-to-ocean fluxes. The only fluxes calculated from simultaneously measured  $\text{NH}_3$  (g) and  $\text{NH}_x$  (s) concentrations were for the North Sea (Asman et al. 1994) where values ranged from  $-75$  to  $43 \mu\text{mol m}^{-2} \text{d}^{-1}$ . The net direction of the flux depends primarily on the highly variable  $(\text{NH}_3)_g$  as for

other regions under continental influence. Fluxes derived from the measured concentration data were either more negative or more positive than those derived from the modeled concentrations. This difference could be due to sampling artifacts, inadequacies in the models, or difficulties in comparing discrete and time-averaged fluxes.

Sensitivity tests indicate that the flux estimates depend strongly on changes in the seawater  $\text{NH}_x$  and atmospheric  $\text{NH}_3$  concentrations. Therefore, to define the role of oceanic ammonia emissions in the nitrogen budget of the North Atlantic Basin, simultaneous and accurate measurements of  $(\text{NH}_3)_g$  and  $[\text{NH}_x]_s$  in several regions are needed. These should be compared to model-derived values over equivalent spatial and temporal scales for validation of the models. The eventual goal is to develop models which are able to simulate accurately the nitrogen dynamics of the North Atlantic Basin. Such models will help to determine the magnitude of oceanic  $\text{NH}_3$  emissions on a regional basis, the influence of continental  $\text{NH}_3$  emissions on the North Atlantic Basin, and the regional effects of  $\text{NH}_3$  on aerosol chemical, physical, and optical properties in the North Atlantic atmosphere.

## Acknowledgments

We would like to acknowledge W. Asman for supplying the compensation point calculation method used in the MSC-W model and W. Asman and T. Bates for comments on the manuscript. We thank the organizers of the Block Island workshop (R. Howarth and J. Galloway) for providing the forum that inspired this joint effort. We also appreciate the funding provided by UNEP and the Mellon Foundation to support the efforts of the SCOPE Nitrogen Project and by the World Meteorological Organization to investigate the interaction between the N cycles of the atmosphere and the North Atlantic Ocean. Work done by P. K. Quinn was funded by the NOAA Climate and Global Change Program. Work done by K. J. Barrett was supported by the Department of the Environment of the United Kingdom and was a voluntary contribution-in-kind to EMEP. Work done by K. D. Six was supported by EC under Contract EV5V-CT92-0124. Work done by F. Lipschultz was supported by NSF grant # OCE90-16069. This is PMEL contribution number 1609 and BBSR contribution number 1406.

## References

- Asman WAM, Drukker B & Janssen AJ, (1988) Modelled historical concentrations and depositions of ammonia and ammonium in Europe. *Atm. Environ.* 22: 725–735

- Asman WAM, Harrison RM & Ottley CJ (1994) Estimation of the net air-sea flux of ammonia over the Southern Bight of the North Sea. *Atm. Environ.* 28: 3647–3654
- Bates RG & Pinching GD (1950) Dissociation constants of aqueous ammonia at 0 to 50 C from e.m.f. studies of the ammonium salt of a weak acid. *J. Am. Chem. Soc.* 72: 1393–1396
- Brzezinski MA (1988) Vertical distribution of ammonium in stratified oligotrophic waters. *Limnol. Oceanogr.* 33: 1176–1182
- Brockmann UH, Laane RWPM & Postma H (1990) Cycling of nutrient elements in the North Sea. *Netherlands J. of Sea Res.* 26: 239–264
- Buijsman E, Maas HFM & Asman WAH (1987) Anthropogenic NH<sub>3</sub> emission in Europe. *Atm. Environ.* 21: 1009–1022
- Carpenter EJ (1973) Nitrogen fixation by *Oscillatoria (Trichodesmium) theibautii* in the south-western Sargasso Sea. *Deep-Sea Res.* 20: 285–288
- Carpenter EJ & McCarthy JJ (1975) Nitrogen fixation and uptake of combined nitrogenous nutrients by *Oscillatoria (Trichodesmium) theibautii* in the western Sargasso Sea. *Limnol. Oceanogr.* 20: 389–401
- Clarke AD & Porter JN (1993) Pacific marine aerosol 2. Equatorial gradients in chlorophyll, ammonium, and excess sulfate during SAGA-3. *J. Geophys. Res.* 98: 16997–17010
- Cochlan (1986) Seasonal study of uptake and regeneration of nitrogen on the Scotian Shelf. *Cont. Shelf Res.* 5: 555–577
- Dasgupta PK & Dong S (1986) Solubility of ammonia in liquid water and generation of trace levels of standard gaseous ammonia. *Atm. Environ.* 20: 565–570
- D'Elia CF (1983) Nitrogen determination in seawater. In: Carpenter EJ & Capone DG (Eds) *Nitrogen in the Marine Environment* (pp 731–762). Academic Press, New York
- Dentener FJ & Crutzen PJ (1994) A three dimensional model of the global ammonia cycle. *J. Atm. Chem.* 19: 331–369
- Duce RA, Liss PS, Merrill JT, Atlas EL, Buat-Menard P, Hicks BB, Miller JM, Prospero JM, Arimoto R, Church TM, Ellis W, Galloway JN, Hansen L, Jickells TD, Knap AH, Reinhardt KH, Schneider B, Soudine A, Tokos JJ, Tsunogai S, Wollast R & Zhou M (1991) The atmospheric input of trace species to the world ocean. *Global Biogeochem. Cycles* 5: 193–260
- Garrels RM & Christ CL (1965) *Solutions, Minerals, and Equilibria*. Harper and Row, New York
- Garside C & Garside JC (1993) The “f-ratio” on 20W during the North Atlantic Bloom Experiment. *Deep-Sea Res.* 40: 75–90
- Georgii HW & Gravenhorst G (1977) The ocean as a source or sink of reactive trace gases. *Pageoph.* 115: 503–511
- Glibert PM, Dennett MR & Caron DA (1988) Nitrogen uptake and ammonium regeneration by pelagic microplankton and marine snow from the North Atlantic. *J. Mar. Res.* 46: 837–852
- Glibert PM & McCarthy JJ (1984) Uptake and assimilation of ammonium and nitrate by phytoplankton: Indices of nutritional status for natural assemblages. *J. Plankton Res.* 6: 677–697
- Hanson RB & Robertson CY (1988) Spring recycling rates of ammonium in turbid continental shelf waters off the southeastern United States. *Cont. Shelf Res.* 8: 49–68
- Harrison WG (1983) The time-course of uptake of inorganic and organic nitrogen compounds by phytoplankton from the Eastern Canadian Arctic: A comparison with temperate and tropical populations. *Limnol. Oceanogr.* 28: 1237–1242
- Harrison WG, Head EJH, Home EPW, Irwin B, Li WKW, Longhurst AR, Paranjape MA & Platt T (1993) The western North Atlantic Bloom Experiment. *Deep-Sea Res.* 40: 279–305
- Jones RD (1991) An improved fluorescence method for the determination of nanomolar concentrations of ammonium in natural seawaters. *Limnol. Oceanogr.* 36: 814–819
- Kurz KD (1993) Zur saisonalen Variation des ozeanischen Kohlendioxidpartialdrucks, Examensarbeit Nr. 18. Max-Planck-Institut fuer Meteorologie
- Kurz KD & Dentener FJ (1994) Exchange of dimethylsulfide and ammonia between the ocean and the atmosphere calculated using a global ocean and atmospheric model. (in preparation)

- Lancelot C, Mathot S & Owens NJP (1986) Modelling protein synthesis, a step to an accurate estimate of net primary production: *Phaeocystis pouchetii* colonies in Belgium coastal waters. *Marine Ecol. Prog. Ser.* 32: 193–202
- LeBel PJ, Hoell JM, Levine JS & Vay SA (1985) Aircraft measurements of ammonia and nitric acid in the lower troposphere. *Geophys. Res. Lett.* 12: 401–404
- Le Bouteiller A (1986) Environmental control of nitrate and ammonium uptake by phytoplankton in the equatorial Atlantic Ocean. *Marine Ecol. Prog. Ser.* 30: 1647–1679
- Liss PS & Galloway JN (1993) Air-sea exchange of sulfur and nitrogen and their interaction in the marine atmosphere. In: Wollast R, Mackenzie FT & Chou L (Eds) *Interactions of C, N, P, and S Biogeochemical Cycles and Global Change* (pp 259–281). Springer-Verlag, Berlin
- Longhurst AR, Bedo A, Harrison WG, Head EJH, Horne EP, Irwin B & Morales C (1989) NFLUX: A test of vertical nitrogen flux by diel migrant biota. *Deep-Sea Res.* 36: 1705–1721
- Lyman J & Fleming RH (1940) Composition of seawater. *J. Mar. Resources* 3: 134–146
- Maier-Reimer E (1993) Geochemical cycles in an ocean general circulation model: Preindustrial tracer distributions. *Global Biogeochem. Cycles* 7: 645–677
- Pickard GL & Emery WJ (1982) *Descriptive Physical Oceanography, An Introduction*. Pergamon Press, New York, 44 p
- Quinn PK, Charlson RJ & Zoller WH (1987) Ammonia, the dominant base in the remote marine troposphere: A review. *Tellus* 39B: 413–425
- Quinn PK, Charlson RJ & Bates TS (1988) Simultaneous observations of ammonia in the atmosphere and ocean. *Nature* 335: 336–338
- Quinn PK, Bates TS, Johnson JE, Covert DS & Charlson RJ (1990) Interactions between the sulfur and reduced nitrogen cycles over the central Pacific Ocean. *J. Geophys. Res.* 95: 16405–16416
- Quinn PK, Asher WE & Charlson RJ (1992) Equilibria of the marine multiphase ammonia system. *J. Atmos. Chem.* 14: 11–30
- Seinfeld JH (1986) *Atmospheric Chemistry and the Physics of Air Pollution*. Wiley, New York
- Slawyk G & MacIsaac JJ (1972) Comparison of two automated ammonium methods in a region of coastal upwelling. *Deep-Sea Res.* 19: 521–524
- Taylor AH & Stevens JA (1980) Seasonal and year-to-year variations in surface salinity at the nine North Atlantic Ocean weather stations. *Ocean. Acta* 3: 421–429
- Tuovinen JP, Barrett KJ & Styve H (1994) Transboundary acid pollution in Europe: Calculated fields and budgets 1985–1993, EMEP/MSC-W Report 1/94. Norwegian Meteorological Institute, Oslo
- Warneck P (1988) *Chemistry of the Natural Atmosphere*. Academic Press, San Diego, CA, pp 426–441
- Williams EJ, Sandholm ST, Bradshaw JD, Schendel JS, Langford AO, Quinn PK, LeBel PJ, Vay SA, Roberts PD, Norton RB, Watkins BA, Buhr MP, Parrish DD, Calvert JG & Fehsenfeld FC (1992) An intercomparison of five ammonia measurement techniques. *J. Geophys. Res.* 97: 11591–11611
- Zhuang L & Huebert B (1994) personal communication.